

## RESEARCH ARTICLE

## Lunar tides in total electron content over Brazil

10.1002/2017JA024052

## Key Points:

- Lunar diurnal and semidiurnal tides have been observed in TEC over Brazil
- The amplitudes of the lunar semidiurnal tide were large during SSW events
- The amplitudes of the lunar semidiurnal tide had maximum over the EIA crest and minimum following the magnetic equator

## Correspondence to:

A. R. Paulino,  
arspaulino@gmail.com

## Citation:

Paulino, A. R., L. M. Lima, S. L. Almeida, P. P. Batista, I. S. Batista, I. Paulino, H. Takahashi, and C. M. Wrasse (2017), Lunar tides in total electron content over Brazil, *J. Geophys. Res. Space Physics*, 122, 7519–7529, doi:10.1002/2017JA024052.

Received 17 FEB 2017

Accepted 18 JUN 2017

Accepted article online 20 JUN 2017

Published online 4 JUL 2017

A. R. Paulino<sup>1,2</sup> , L. M. Lima<sup>1</sup> , S. L. Almeida<sup>1</sup> , P. P. Batista<sup>3</sup> , I. S. Batista<sup>3</sup> , I. Paulino<sup>2</sup> , H. Takahashi<sup>3</sup> , and C. M. Wrasse<sup>3</sup> 

<sup>1</sup>Departamento de Física, Universidade Estadual da Paraíba, Campina Grande, Brazil, <sup>2</sup>Unidade Acadêmica de Física, Universidade Federal de Campina Grande, Campina Grande, Brazil, <sup>3</sup>Divisão de Aeronomia, Instituto Nacional de Pesquisas Espaciais, São José dos Campos, São Paulo, Brazil

**Abstract** Using data from Global Navigation Satellite Systems dual frequency receivers, the lunar tides were studied in the ionospheric total electron content (TEC) over Brazil from 2011 to 2014. In order to calculate the amplitudes and phases of the lunar tides, quiet magnetic days within a 27 day (window) have been used to remove the solar rotation effects. Relative residuals TEC were calculated by performing a spectral analysis by removing the solar tide contributions. Lastly, a lunar month size window was used to calculate the amplitude and phase of the lunar components. Lunar diurnal tide amplitudes showed a semiannual variation with maximum in the equinox months for almost all latitudes, while lunar semidiurnal amplitudes were larger in December and January and may be related to sudden stratospheric warming events. Both components did not display significant longitudinal variation what could be due to the short range of longitude (30°). Lunar diurnal amplitudes were basically uniform over Brazil, while lunar semidiurnal amplitudes showed some peaks over the equatorial ionization anomaly crest and minimum values near the magnetic equator.

## 1. Introduction

The atmospheric lunar tide is produced primarily by the gravitational forces acting on the Earth-ocean-atmosphere system. Lunar tide in the atmosphere has small amplitudes when compared to the solar tide. However, this oscillation is interesting due to the well-known forcing, quite regularly distributed over the Earth and predictable. Even so, a strong temporal variability of the lunar tide in the atmosphere along the time has been observed, which cannot be attributed to the lunar tidal potential variation and must be due to changes in the background atmosphere. Thus, the studies on the lunar tide can be used to investigate variations in the atmosphere for medium- and long-term periods.

The most important component of the lunar tide is the  $M_2$  with period of 12.42 h [e.g., Haurwitz and Cowley, 1969; Stening and Vincent, 1989; Forbes, 1982; Pedatella et al., 2012a]. Secondary contributions of the diurnal component with period of 24.84 h have also been observed [e.g., Matsushita, 1967a; Pedatella and Forbes, 2010].

Studies of atmospheric lunar tide started using barometric data on Earth surface in 1847 where signature of the atmospheric lunar tide was observed in the pressure measurements at St. Helena observatory [Sabine, 1847]. In the mesosphere and lower thermosphere (MLT), radar measurements were largely used to study the lunar tide around the world [e.g., Stening et al., 1990, 1994, 2003; Niu et al., 2005; Sandford and Mitchell, 2007; Sandford et al., 2007, Paulino et al., 2012a, 2015]. More recently, satellite data have been used to investigate the global structure of the lunar tide [e.g., Forbes et al., 2013, Paulino et al., 2013].

Recently, researches on the lunar tide have pointed out that the enhancement of the lunar tide and changes in the ionosphere dynamics may be related to sudden stratospheric warming (SSW) events [Chau et al., 2009; Fejer et al., 2010; Yamazaki, 2013; Pedatella, 2014; Pedatella and Maute, 2015]. Effects of the SSW on the amplitude of the lunar tide in the MLT region have been reported by various authors [e.g., Paulino et al., 2012b; Forbes and Zhang, 2012; Zhang and Forbes, 2014; Chau et al., 2015].

Several works have been published reporting the lunar tide effects in the ionospheric *E* region [e.g., Matsushita, 1956; Wright and Skinner, 1959; Kotadia, 1962; Matsushita, 1967a; Joshi and Kotadia, 1970; Tarpley and Matsushita, 1971, 1972; Stening, 2011] and in the *F* region parameters [e.g., Abur-Robb and Dunford, 1975; Stening and Fejer, 2001; Chau et al., 2009; Eccles et al., 2011; Fejer et al., 2010, 2011]. Magnetometer measurements have been used as well to study the characteristics of the lunar tide using variations in the ionospheric electric

currents [e.g., *Bartels and Johnston*, 1940; *Matsushita and Maeda*, 1965; *Matsushita*, 1967b]. The lunar tide has also been studied using the total electron content (TEC) [*Bernhardt et al.*, 1976; *Bhuyan and Tyagi*, 1986; *Pedatella and Forbes*, 2010; *Pedatella et al.*, 2012b; *Pedatella and Maute*, 2015].

*Chau et al.* [2009] reported large semidiurnal perturbations on the *F* region vertical plasma drifts over Jicamarca (11.9°S, 76.8°W) during the sudden stratospheric warming event that occurred in January 2008. *Fejer et al.* [2010] reported that these perturbations are preceded by large dayside downward drifts and westward equatorial electrojet currents and proposed that those variations are due to enhanced lunar tidal effects. *Liu et al.* [2011] showed that the contrast between the dip equator and low latitude in the TEC response in the Asian sector during a sudden stratospheric warming in 2009 was in agreement with the latitudinal structure of the lunar semidiurnal tide. *Fejer et al.* [2011] reported very strong enhanced lunar semidiurnal vertical plasma drift amplitudes during early morning during low solar flux conditions over Jicamarca.

*Eccles et al.* [2011] combined the Huancayo magnetometer data, Jicamarca ionosonde data, and ionosphere electrodynamics model to demonstrate the large modulation of the vertical plasma drift during low solar activity. They concluded that the lunar tide is an important and predictable component of low-latitude ionosphere variability during low solar activity. Besides, they suggest that the identification of a well-defined variation of the neutral wind field, zonal electric field, and vertical plasma drift related to lunar tides will provide better model drivers and reduce the unknown portions of the day-to-day weather in the low-latitude ionospheric drivers.

The present work aims to study the lunar tide over Brazil using TEC data from a network of Global Navigation Satellite Systems (GNSS) receivers. The main motivation for the present study is that the Brazilian region has two important anomalies that contribute to the complex structure and dynamics of its ionosphere: (1) the presence of the South Atlantic/America Magnetic Anomaly and (2) the high magnetic declination in most part of the country. Those characteristics are unique around the world; thus, the understanding of the lunar tide must be useful to understand the coupling between neutral and ionized parts of the atmosphere. Other interesting aspect of the present research is that the Brazilian area covers the magnetic equator and the south peak of the equatorial ionization anomaly (EIA), then comparative effects can be investigated in details. For the present study 4 years of data, from January 2011 to December 2014, were used.

## 2. Data and Methodology

TEC data used in this work were provided by the Brazilian Study and Monitoring of Space Weather Program (EMBRACE-“Estudo e Monitoramento Brasileiro de Clima Espacial”) of the National Institute for Space Research (INPE-“Instituto Nacional de Pesquisas Espaciais”). They provide ionospheric TEC maps for the Brazilian territory with 10 min time resolution obtained continuously during day and night [*Takahashi et al.*, 2015, 2016]. The TECMAPs are available online at the EMBRACE website (<http://www2.inpe.br/climaespacial>).

The GNSS network is maintained and operated by the Brazilian Institute of Geography and Statistics (IBGE-“Instituto Brasileiro de Geografia e Estatística”). The spatial distribution of the receivers is not uniform. Further details on the distribution of the receiver can be found in *Takahashi et al.* [2014], and the detailed methodology on how to estimate the TECMAPs from the GNSS signal over Brazil was published by *Takahashi et al.* [2016].

TECMAPs were calculated with horizontal cells of  $0.5^\circ \times 0.5^\circ$  in latitude and longitude. In order to optimize the spatial resolution of the Brazilian TECMAPs, an algorithm based on the methodology developed by *Otsuka et al.* [2002] was developed. TECMAPs were first calculated and averaged inside an area of  $160 \times 160 \text{ km}^2$  correspondent to  $3 \times 3$  cells. If no data are found, the running average area goes to  $260 \times 260 \text{ km}^2$  ( $5 \times 5$  cells). This procedure is repeated up to an area of  $1000 \times 1000 \text{ km}^2$  ( $21 \times 21$  cells), in an extreme case. According to *Takahashi et al.* [2016], over Brazil, most of the data point of TEC were obtained using a running average of less than 11 elements, i.e., on average, the spatial resolution was approximately 50 to 100 km in the southeastern part of Brazil, 200–300 km in the northeastern part, and greater than 500 km in the Amazon region. Figure 1 shows the diurnal variation of the TEC over Brazil calculated for 1 October 2012 every 6 h (Figures 1a–1d) and for 1 October 2014 (Figures 1e–1h). Although after 2013 other GNSS network receivers were included to the calculations of TECMAPs covering practically the entire South American continent, in the present work, only data over the Brazilian area were used in order to have a long-term database.

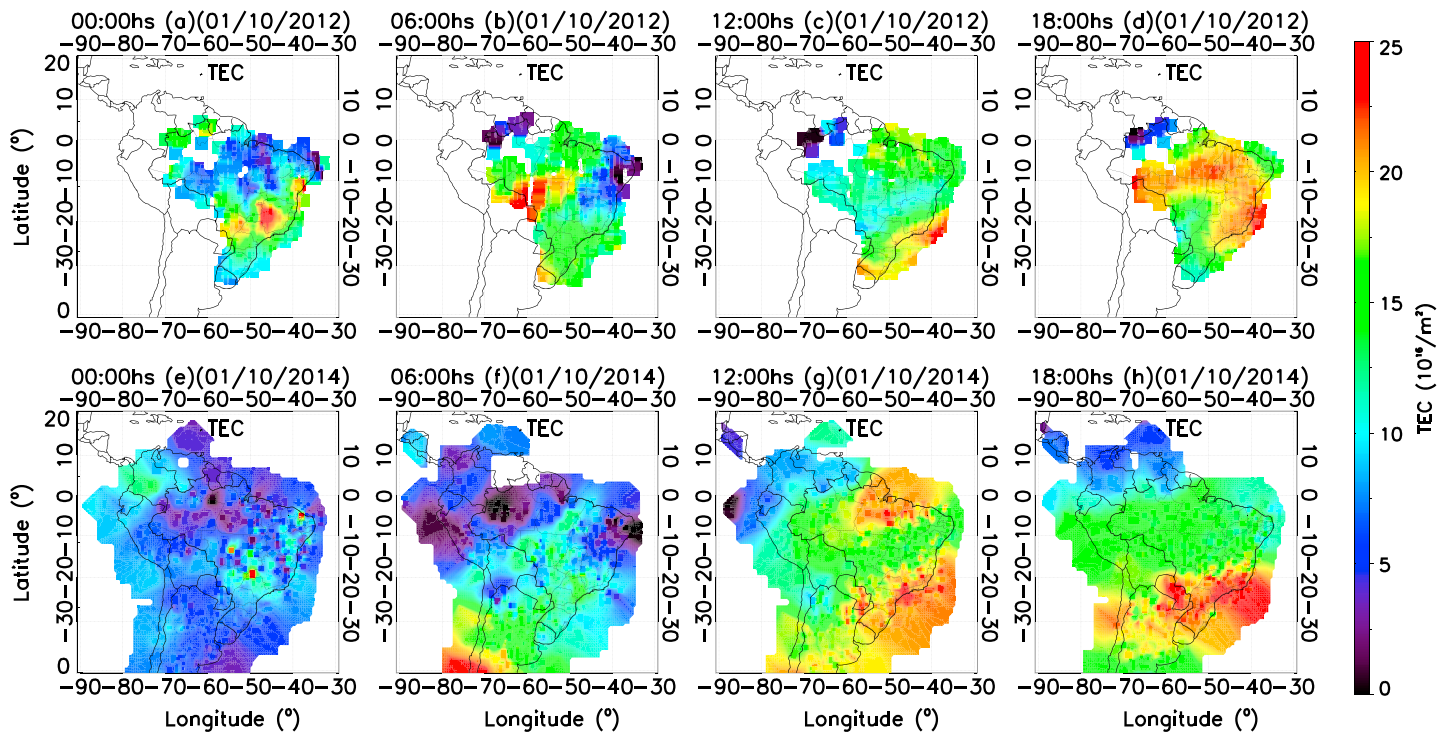


**Figure 1.** TECMAPs calculated over Brazil on 1 October 2012 at (a) 00:00 UT, (b) 06:00 UT, (c) 12:00 UT, and (d) 18:00 UT and on 1 October 2014 at (e) 00:00 UT, (f) 06:00 UT, (g) 12:00 UT, and (h) 18:00 UT. Colors represent the TEC units ( $10^{16}$  el/m<sup>2</sup>).

Determination of the lunar tide in TEC map data requires a careful analysis because the amplitude of the lunar tide is small compared to the solar tide. In this work, the lunar tide calculations followed the methodology of *Pedatella and Forbes* [2010]. Only geomagnetic quiet days ( $K_p < 3$ ) were used. After the elimination of geomagnetic effect, a Fourier analysis was performed to calculate the subharmonic of the solar day (diurnal, semidiurnal, and terdiurnal) with a 27 day window. The 27 day window was used to eliminate the solar rotation effects, and the 27 day window was moved forward 1 day at time to calculate the mean solar day variation centered in the window. Residuals from the solar daily variation are subsequently divided by the mean level in order to obtain relative residuals. Using relative residuals, it is possible to combine multiple years of observation to calculate the lunar tide removing possible effects of the solar cycle and seasonal variations.

Using the residual signals, components of the lunar tide were obtained applying a least squares analysis in a window of 29 day, which corresponds to a lunar month. The least squares method uses the following equation for the residual signal:

$$y(\tau) = \sum_{n=0}^2 A_n \cos(n\tau + \phi_n), \tag{1}$$

where  $\tau$  is the lunar time and  $A_n$  and  $\phi_n$  represent the amplitude and phase, respectively, for  $n$  subharmonics of the lunar day (24.83 h). The lunar time is calculated as

$$\tau = t - \nu, \tag{2}$$

where  $t$  is the solar time and  $\nu$  is the age of the Moon (cyclic term which is dependent on the phase of the Moon and where  $\nu = 0$  is equivalent to new moon). Lastly, representative years of the lunar tide amplitudes were vector averaged for the 4 years of data.

Figure 2 shows evidences of the semidiurnal (a) and diurnal (b) lunar tide in the TEC data observed at 46°W and 23°S, during two different lunar months. Notice that Figure 2a shows two oscillations in the lunar composite day, while for Figure 2b the main oscillation has only one cycle. Figure 2c shows the strength of the semidiurnal component in the residual signal, while Figure 2d is for the diurnal case.

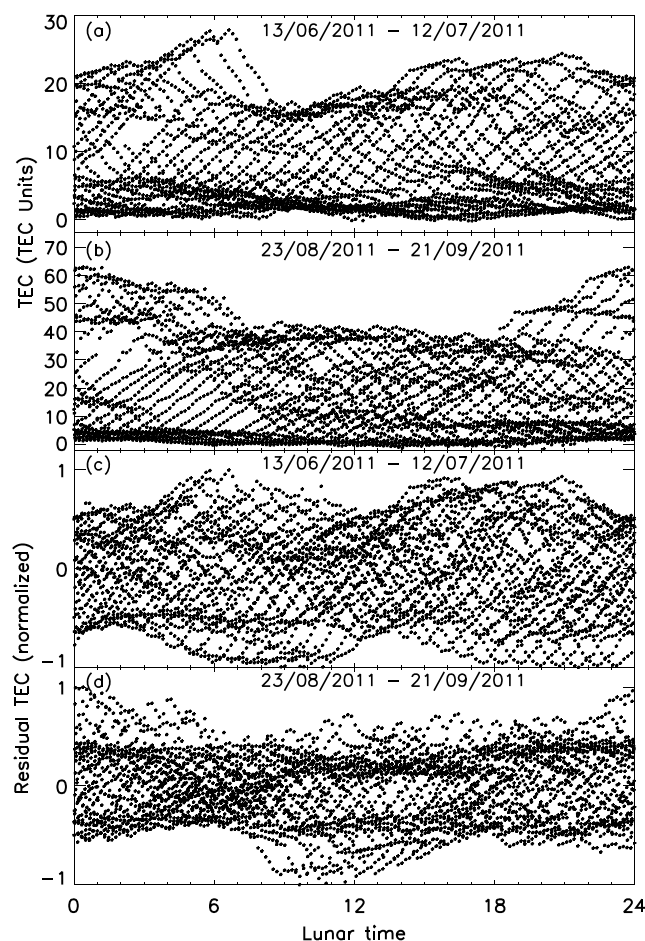


**Figure 2.** (a and b) TEC and (c and d) relative residual TEC observed at  $46^{\circ}\text{W}$  and  $23^{\circ}\text{S}$ . Figures 2a and 2c were observed from 13 June to 12 July 2011 and show evidences of the lunar semidiurnal tide. Figures 2b and 2d were observed from 23 August to 21 September 2011 and show evidences of the lunar diurnal tide.

### 3. Results and Discussions

Figure 3 shows the zonal vector average for the amplitudes of the lunar semidiurnal (top) and diurnal (bottom) tides calculated over all the observed period (2011–2014) as a function of the time of the year and magnetic latitude. The amplitudes were calculated as percentage of the total variation of the TEC excluding the solar components. Error bars represent the maximum standard deviation along the months for all latitude-longitude ranges. One can see a seasonal and latitudinal variability in the lunar tide amplitudes over the Brazilian sector. The mean amplitudes of the semidiurnal component, between  $5^{\circ}$  and  $15^{\circ}$  magnetic latitudes, were maxima from November to January, and there was a secondary peak in April. The minima values of amplitudes were obtained from May to August, with values lower than 2% of TEC variation. The present results showed a clear seasonal variability in the lunar semidiurnal tide. However, between  $-25^{\circ}$  and  $-5^{\circ}$  is possible to see some peaks in amplitude from December to January, in April, and from September to October. The minima values of the amplitude were observed from May to August. It is possible to notice that the lunar semidiurnal tide amplitudes along the magnetic equator are smaller than at other magnetic latitudes investigated.

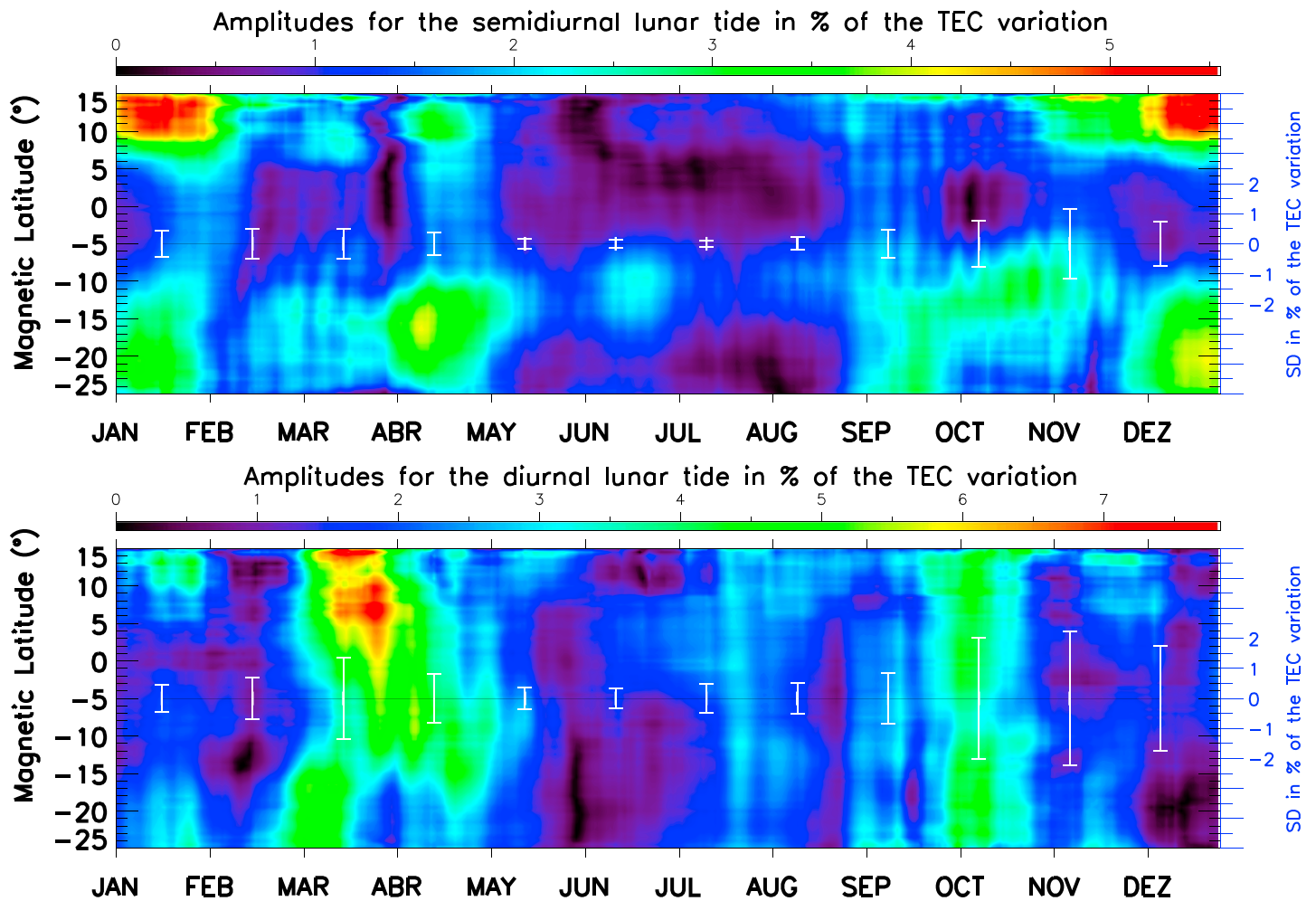
Both the seasonality and the latitudinal structure in the amplitudes of the lunar semidiurnal tide are in agreement with the results of *Pedatella* [2014]. Moreover, the magnitude of the amplitude values agrees with previous works using TEC [*Pedatella and Forbes*, 2010; *Pedatella*, 2014] as well.

Figure 3 shows that the behavior of the diurnal tide is completely different from that of the semidiurnal component. For instance, the latitudinal variation for the diurnal component is less significant than for the semidiurnal tide. The seasonal variation is well defined for all latitudes with maximum in the equinoxes and minimum around the solstice months.

The seasonality of the lunar tide in the ionosphere is well known, and it has been observed elsewhere [*Pedatella et al.*, 2012b; *Pedatella*, 2014]. However, the sources of the seasonality remain without explanation. Several works have reported enhancements of the lunar semidiurnal tide observed at some atmospheric fields in January during the sudden stratospheric warming events [*Forbes and Zhang*, 2012; *Paulino et al.*, 2012b; *Pedatella et al.*, 2012b; *Yamazaki*, 2013; *Chau et al.*, 2015]. This may be the reason for the peak in the lunar semidiurnal tide amplitude observed in December/January.

Figure 4 shows the amplitudes of the semidiurnal (top) and diurnal (bottom) tides for the whole observed period. This plot can be used to investigate the interannual variability of the lunar tide amplitudes. One can see a clearly year to year variability for both components.

During the period of the present study a minor SSW in 2012 and a major SSW in 2013 were observed [*Yamazaki*, 2013]. Some peaks of amplitude for the semidiurnal component in January, except in 2011, can also be seen.



**Figure 3.** Amplitudes of the (top) semidiurnal and (bottom) diurnal lunar tides as a function of magnetic latitude and day of the year. Amplitudes were calculated as variation of the relative residual TEC and ARE shown in the color patterns. The amplitudes were vector averaged from 2011 to 2014. Error bars represent the maximum standard deviation along the months considering all latitude and longitudes investigated.

Those peaks were stronger in the northern magnetic part of Brazil. It is important to notice that the strongest peak of amplitude was observed in January 2013 which is coincident with a major SSW event. In January 2013, the enhancement of the lunar semidiurnal tide amplitudes extended to the southern part as well. It is important to observe that the slightly enhancements were observed in December months as well.

Goncharenko *et al.* [2013] analyzed the major SSW occurred in 2013 and concluded that the ionospheric anomalies associated with this event were observed from December 2012 to January 2013. Besides, they associated the perturbations in the vertical drift and TEC with lunar semidiurnal tide. Maute *et al.* [2016] also investigated the ionosphere during the SSW in 2013 and verified that the features of this atmospheric region were obtained when lunar tides were put in the model.

In 2012, during a minor SSW, the behavior of the amplitude of the lunar semidiurnal tide was quite similar to the 2013; however, the peak amplitude observed in TEC for January was smaller. In January 2014, no SSW event was observed; however, a peak of the lunar semidiurnal tide amplitude was noted only in the northern latitudes (5° to 15°). For January 2011, no enhancement in the amplitudes of the semidiurnal component was detected. Basically, during the observed period, the amplitudes of the lunar semidiurnal tide were smaller near the magnetic equator.

Yamazaki [2013] studied the lunar semidiurnal tide in the equatorial electrojet and observed the enhancement of this oscillation during SSW events. Besides, he concluded that the average amplitude of the

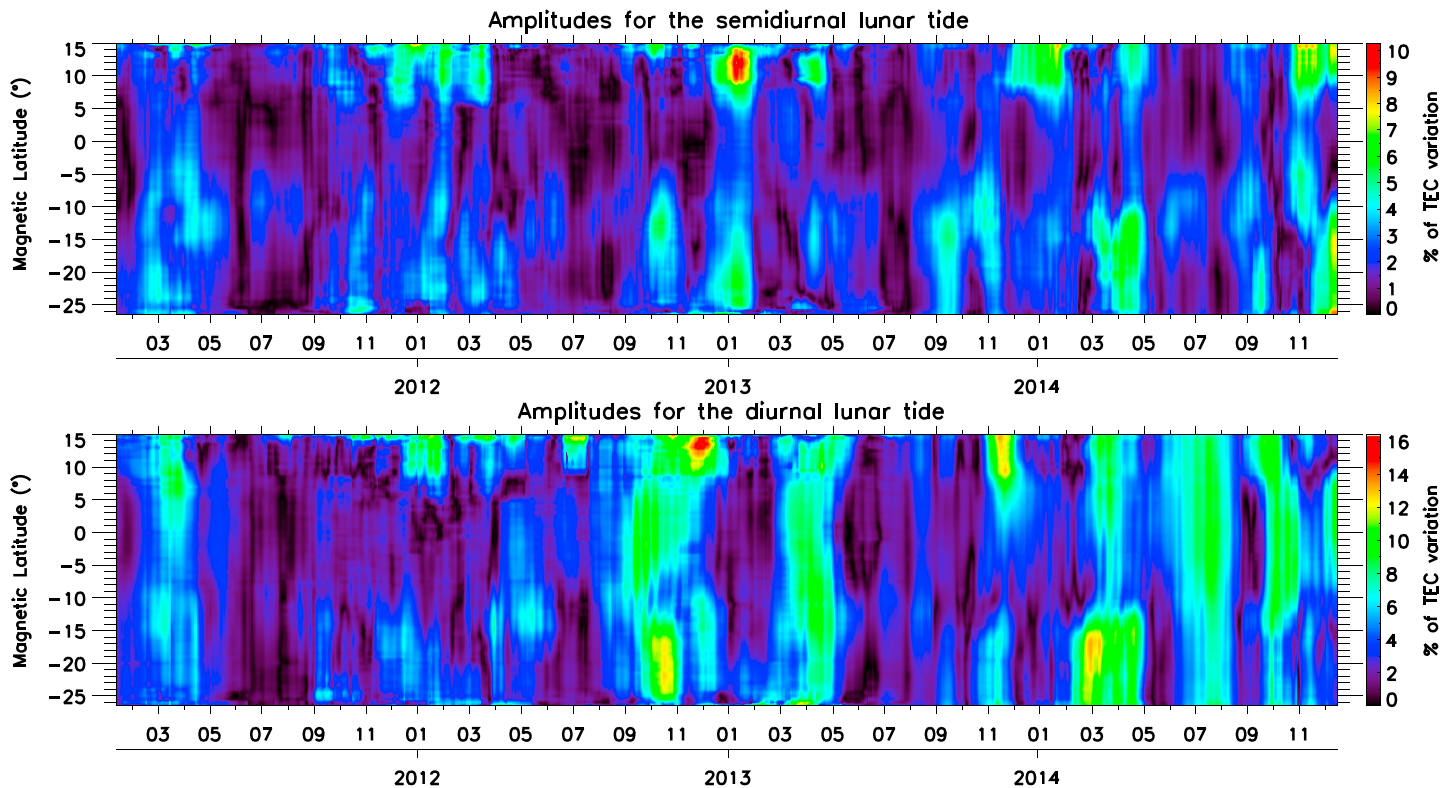


**Figure 4.** Same of Figure 3 but for whole observed period.

semidiurnal component during non-SSW events is still larger than that of the June solstice, indicating that the SSW events are not the only responsible of the lunar tide intensification in December solstice.

Another important aspect to be considered is that the enhancement of the lunar diurnal tide amplitudes did not match with the semidiurnal ones, i.e., the peaks in the amplitude appeared mostly from March to May, except in 2012, and from September to November, except in 2013. In some periods of observation, the diurnal amplitudes were larger than the semidiurnal amplitudes, but, as also observed by *Pedatella and Forbes* [2010].

*Forbes and Zhang* [2012] suggested that the mechanism responsible for the amplification of the lunar semidiurnal tide during 2009 SSW is the Pekeris resonance peak. This mechanism consists in a shift of the  $M_2$  oscillation period, in the atmosphere, due to changes in the zonal mean wind distribution in connection with the SSW. The mechanism was subsequently confirmed for other SSW events by the work of *Zhang and Forbes* [2014].

Figure 5 shows the longitudinal and temporal variation of the semidiurnal (top) and diurnal (bottom) amplitudes for a fixed magnetic latitude  $15^\circ\text{S}$ , which corresponds to the southern crest of the equatorial ionization anomaly. Annual variations in the amplitude of the lunar semidiurnal tide for all period of the study were observed, which is in agreement to the observations of *Pedatella and Forbes* [2010]. Furthermore, for the Brazilian longitudinal sector, a secondary enhancement in most of the equinox months was also noted. Otherwise, the amplitudes of the diurnal tide present a more pronounced semiannual variation with maximum in the equinoxes. One interesting observed aspect was an enhancement in the amplitude for both components from March to May 2014.

*Forbes et al.* [2006] point out that the nonmigrating tides can rise from the following: zonally asymmetric excitation source, by propagation of migrating tides through a zonally asymmetric stationary background atmosphere, and nonlinear interactions or interactions between a zonally asymmetric distribution of gravity waves and the migrating tidal field. *Sandford and Mitchell* [2007] suggested that longitudinal variations observed in the lunar tides signature in the wind field could be attributed to the nonlinear interaction

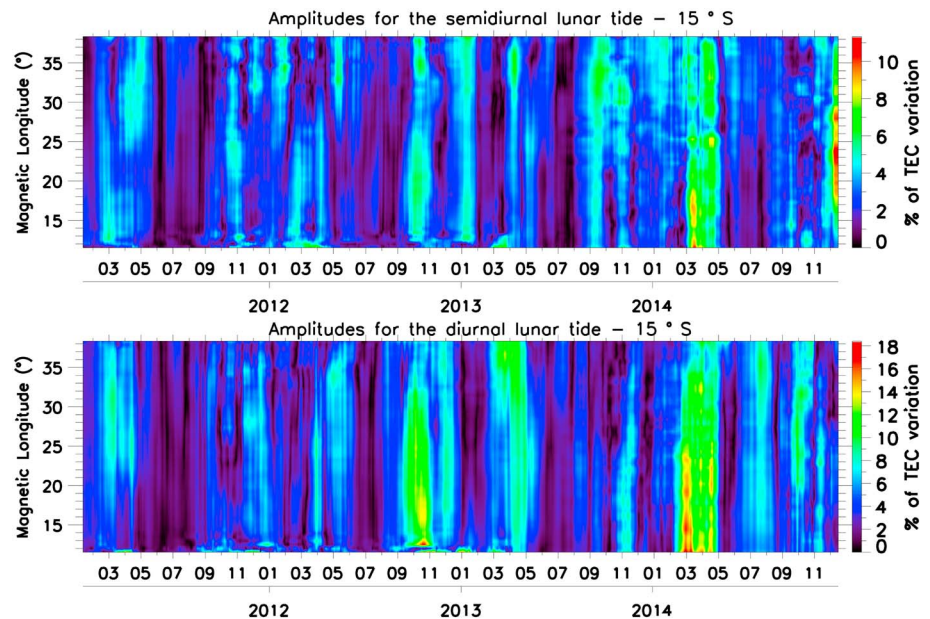


**Figure 5.** Amplitudes of the (top) semidiurnal and (bottom) diurnal lunar tides as a function of longitude and day of the year for a fixed magnetic latitude of  $15^{\circ}$ S. Amplitudes were calculated as variation of the relative residual TEC and are shown in the color patterns.

of stationary planetary waves and migrating tidal components. Besides, nonmigrating components generated due to solid Earth-ocean tidal forcing are known to propagate upward and are capable of producing longitudinal variation in the atmospheric fields, like wind and temperature [Vial and Forbes, 1994]. Thus, the neutral winds may influence the ionospheric dynamo generating electric field, which reveal longitudinal structures in whole ionosphere as shown by Pedatella and Forbes [2010]. Longitudinal structures in the amplitude of the semidiurnal lunar tide were also studied in the MLT region using temperature measurements from the Thermosphere, Ionosphere, Mesosphere Energetics, and Dynamics/Sounding of the Atmosphere using Broadband Emission Radiometry (TIMED/SABER) satellite [Paulino et al., 2013].

Although the previous global studies of the lunar tide have shown longitudinal structures in the amplitudes, in the present work, no evident longitudinal structures were observed; see Figure 5. It may be due to the small longitudinal range ( $30^{\circ}$ ) covered by the TEC measurements over Brazil. According to Pedatella and Forbes [2010], the nonmigrating dominant components which produced the amplitude structures in the semidiurnal component at  $15^{\circ}$ N were S0, SW1, SW3, and SW4. Those modes have long horizontal wavelength and could not be observed in the short longitudinal range of the present work. Furthermore, in the MLT region, the dominant nonmigrating components, which were responsible for the longitudinal structure, were SE3, SE2, SE1, S0, SW1, SW3, SW4, SW5, and SW6 [Paulino et al., 2013]. Even the SW6 component needs a range of  $60^{\circ}$  of longitude, at least, to be observed. Thus, the present results show that if there are longitudinal structures in the amplitude of the semidiurnal and diurnal lunar tides, they may be associated to the components with long horizontal wavelengths.

Figure 6 shows the amplitude of the lunar semidiurnal tide in the TEC variation over the Brazilian area for each month. The results were vector averaged from 2011 to 2014. It is important to note two aspects: (1) the minimum of amplitude is following the magnetic equator along the Brazilian sector and (2) the maximum of amplitude are located at the crest of the EIA. The present results show, in details, how the amplitudes of the lunar semidiurnal tide change along the year over Brazil. For instance, there was a slight motion of the maximum of amplitudes along the year, i.e., in the December solstice (Southern Hemisphere summer), the peak was far from the equator and the amplitudes were larger compared to the June solstice (Southern Hemisphere winter).

Pedatella and Forbes [2010] observed similar characteristics in the global TEC, but they could not give such details for the Brazilian sector; according to them, the maximum of the lunar semidiurnal tide in the EIA crests

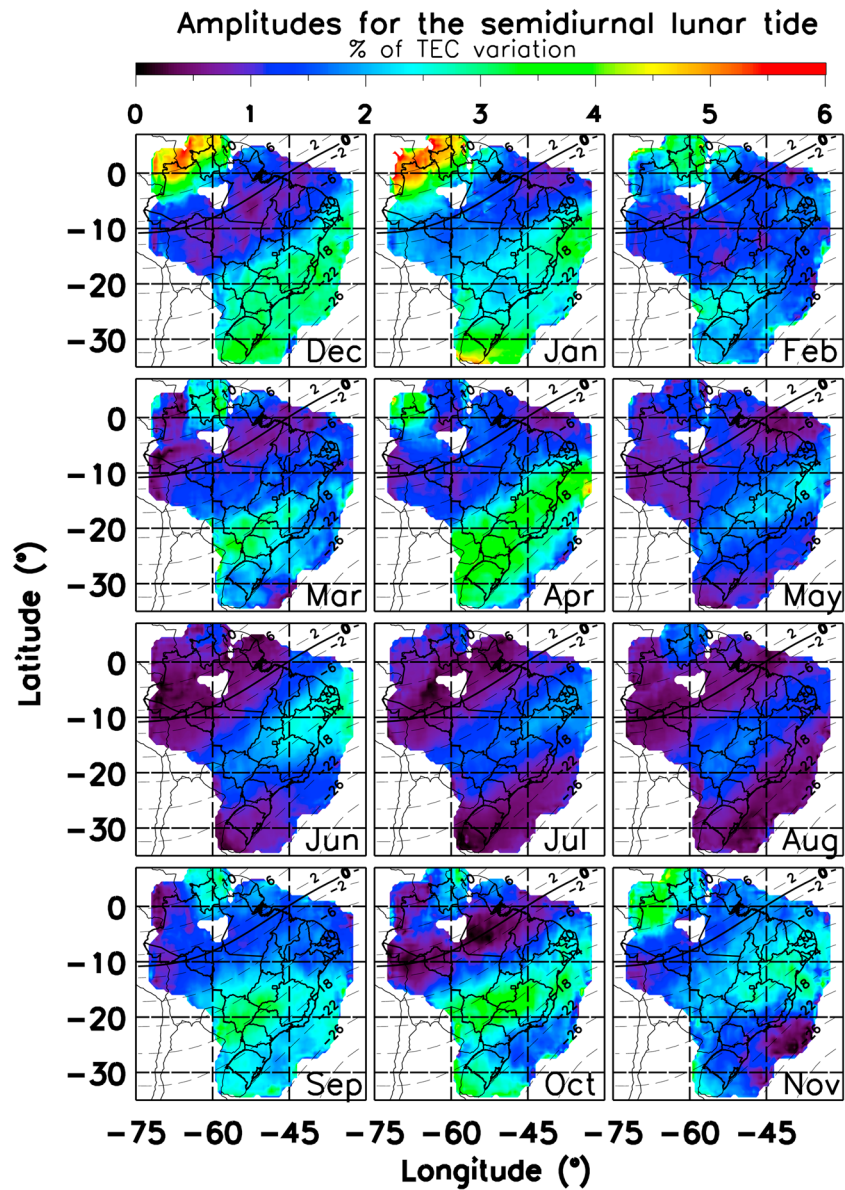


**Figure 6.** Amplitudes of the semidiurnal tide in the relative residual TEC for each month over Brazil.

occurs because of the lunar tide modulation is in the strength of the dynamo generated low-latitude electric field. *Pedatella* [2014] simulated the global characteristics for the lunar tide in TEC, and their results are in agreement with the present observations, i.e., it is expected a minimum of the semidiurnal lunar tide amplitudes near the equator and maximum over the EIA crests in both hemispheres. He also pointed out that the EIA is generated by equatorial electric fields, so the lunar tide in TEC is produced mainly by electrodynamic processes in the ionosphere.

Figure 7 shows the amplitude for the diurnal lunar tide in the TEC. The results were calculated in the same way as for Figure 6. One can note that the diurnal component is more uniform over Brazil. A semiannual variation with maximum in March/April and October and minimum in December and June is clear, primarily, in the southern part of Brazil. Comparing the semidiurnal and diurnal components, the behavior of the amplitudes is completely different. *Pedatella and Forbes* [2010] observed the diurnal lunar tide as well; however, there are few studies about this oscillation in the ionosphere and the mechanism of generation is poorly understood. For instance, *Tarpley* [1971] pointed out the ocean tide as a likely source for the diurnal lunar tide in the atmosphere.

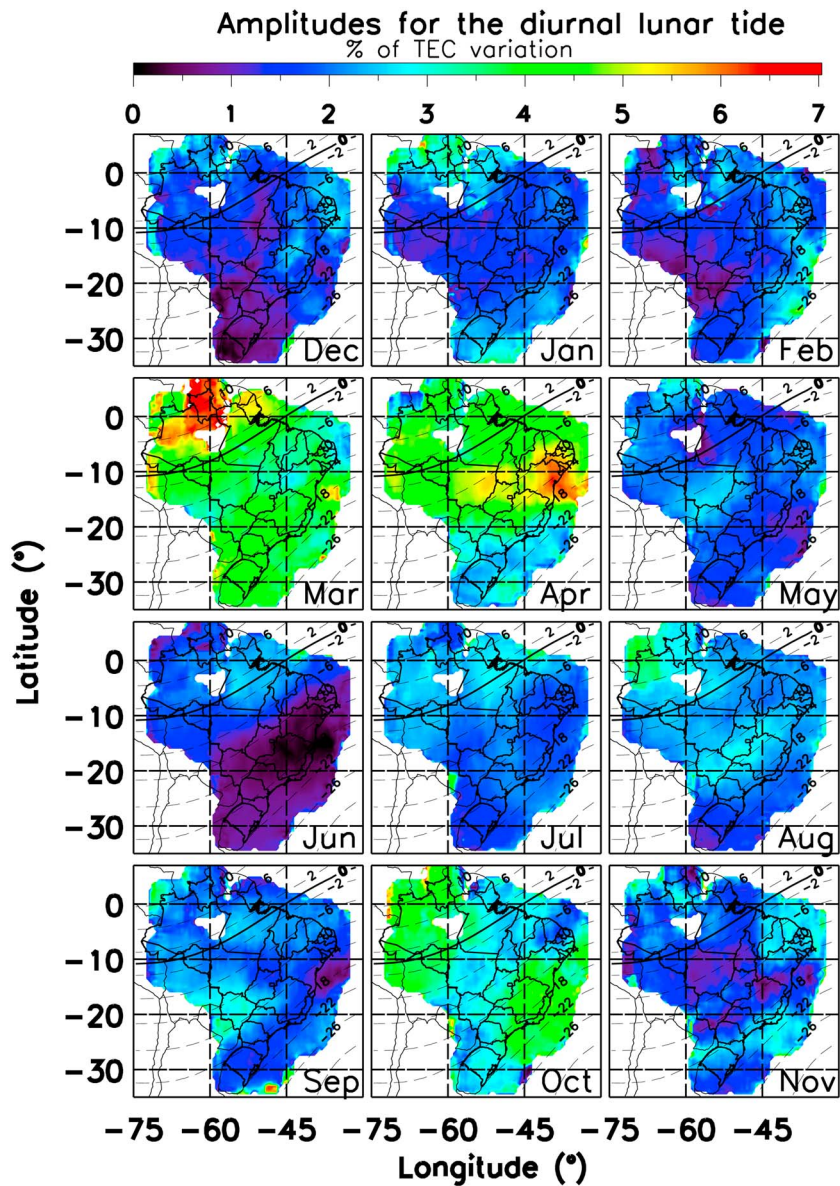


Figure 7. Amplitudes of the diurnal tide in the relative residual TEC for each month over Brazil.

#### 4. Conclusions

TECMAPs obtained from the GNSS receivers were used to study the lunar tide over the Brazilian territory from 2011 to 2014. Amplitudes for the diurnal and semidiurnal components reached up to 6–7% of the TEC variation after removing the solar contributions. Amplitudes for the diurnal tide revealed a well-defined seasonal behavior with maximum in the equinox months. On the other hand, amplitudes for the semidiurnal tide were larger in December–January. In this case, the SSW events of the Northern hemisphere can be pointed as one of the mechanisms responsible for the semidiurnal lunar tide enhancement. Both components did not present significant longitudinal variation in their amplitudes. Since the covered area is only 30° in longitude, these results suggest that nonmigrating component with wave number less than 7 is responsible for the longitudinal structures in the amplitude of the lunar tide. Finally, maxima amplitudes over the EIA crest and minima amplitudes near the magnetic equator for the semidiurnal component were observed. Otherwise, for the diurnal component, the amplitudes were more uniform over Brazil.

### Acknowledgments

The present work was supported by the Coordenação Aperfeiçoamento de Pessoa de Nível Superior (Capes-Brazil) and Conselho Nacional de Desenvolvimento Científico e Tecnológico (CNPq-Brazil) under contracts 166286/2013-3, 460624/2014-8, 310926/2014-9, and 478117/2013-2. The authors thank the EMBRACE program of INPE that kindly supplied the TECMAPs. The data used in this work are available online in the EMBRACE website (<http://www2.inpe.br/climaespacial>).

### References

- Abur-Robb, M. F. K., and E. Dunford (1975), A theoretical evaluation of the lunar tidal variations in the ionospheric  $F_2$ -layer, *Planet. Space Sci.*, *23*, 1071–1080.
- Bartels, J., and H. F. Johnston (1940), Geomagnetic tides in horizontal intensity at Huancayo, *Terr. Magn. Atmos. Electr.*, *45*(3), 269–308, doi:10.1029/TE045i003p00269.
- Bernhardt, P. A., D. A. Antoniadis, and A. V. Da Rosa (1976), Lunar perturbations in columnar electron content and their interpretation in terms of dynamo electrostatic fields, *J. Geophys. Res.*, *81*(34), 5957–5963, doi:10.1029/JA081i034p05957.
- Bhuyan, P., and T. Tyagi (1986), Lunar and solar daily variations of ionospheric electron content at Delhi, *J. Atmos. Terr. Phys.*, *48*(3), 301–310, doi:10.1016/0021-9169(86)90106-6.
- Chau, J. L., B. G. Fejer, and L. P. Goncharenko (2009), Quiet variability of equatorial  $E \times B$  drifts during a sudden stratospheric warming event, *Geophys. Res. Lett.*, *36*(5), L05101, doi:10.1029/2008GL036785.
- Chau, J. L., P. Hoffmann, N. M. Pedatella, V. Matthias, and G. Stober (2015), Upper mesospheric lunar tides over middle and high latitudes during sudden stratospheric warming events, *J. Geophys. Res. Space Physics*, *120*, 3084–3096, doi:10.1002/2015JA020998.
- Eccles, V., D. D. Rice, J. J. Sojka, C. E. Valladares, T. Bullett, and J. L. Chau (2011), Lunar atmospheric tidal effects in the plasma drifts observed by the low-latitude ionospheric sensor network, *J. Geophys. Res.*, *116*, A07309, doi:10.1029/2010JA016282.
- Fejer, B. G., M. E. Olson, J. L. Chau, C. Stolle, H. Lühr, L. P. Goncharenko, K. Yumoto, and T. Nagatsuma (2010), Lunar-dependent equatorial ionospheric electrodynamic effects during sudden stratospheric warmings, *J. Geophys. Res.*, *115*, A00G03, doi:10.1029/2010JA015273.
- Fejer, B. G., B. D. Tracy, M. E. Olson, and J. L. Chau (2011), Enhanced lunar semidiurnal equatorial vertical plasma drifts during sudden stratospheric warmings, *Geophys. Res. Lett.*, *38*, L21104, doi:10.1029/2011GL049788.
- Forbes, J. M. (1982), Atmospheric tide: 2. The solar and lunar semidiurnal components, *J. Geophys. Res.*, *87*(A7), 5241–5252, doi:10.1029/JA087iA07p05241.
- Forbes, J. M., and X. Zhang (2012), Lunar tide amplification during the January 2009 stratosphere warming event: Observations and theory, *J. Geophys. Res.*, *117*, A12312, doi:10.1029/2012JA017963.
- Forbes, J. M., J. Russell, S. Miyahara, X. Zhang, S. Palo, M. Mlynczak, C. J. Mertens, and M. E. Hagan (2006), Troposphere-thermosphere tidal coupling as measured by the saber instrument on timed during July–September 2002, *J. Geophys. Res.*, *111*, A10S06, doi:10.1029/2005JA011492.
- Forbes, J. M., X. Zhang, S. Bruinsma, and J. Oberheide (2013), Lunar semidiurnal tide in the thermosphere under solar minimum conditions, *J. Geophys. Res. Space Physics*, *118*, 1788–1801, doi:10.1029/2012JA017962.
- Goncharenko, L., J. L. Chau, P. Condor, A. Coster, and L. Benkevitch (2013), Ionospheric effects of sudden stratospheric warming during moderate-to-high solar activity: Case study of January 2013, *Geophys. Res. Lett.*, *40*, 4982–4986, doi:10.1002/grl.50980.
- Haurwitz, B., and D. Cowley (1969), The lunar barometric tide, its global distribution and annual variation, *Pure Appl. Geophys.*, *77*(1), 122–150, doi:10.1007/BF00876008.
- Joshi, B. K., and K. M. Kotadia (1970), Lunar tidal variations in the equatorial sporadic-E-layer, *J. Atmos. Terr. Phys.*, *32*, 1057–1066.
- Kotadia, K. M. (1962), The equatorial sporadic-E layer and the electrojet, *J. Atmos. Terr. Phys.*, *24*, 211–218.
- Liu, H., M. Yamamoto, S. Tulasi Ram, T. Tsugawa, Y. Otsuka, C. Stolle, E. Doornbos, K. Yumoto, and T. Nagatsuma (2011), Equatorial electrodynamic and neutral background in the Asian sector during the 2009 stratospheric sudden warming, *J. Geophys. Res.*, *116*, A08308, doi:10.1029/2011JA016607.
- Matsushita, S. (1956), Lunar effects on the equatorial  $E_s$ , *J. Atmos. Terr. Phys.*, *10*, 163–165.
- Matsushita, S. (1967a), Lunar tides in the ionosphere, in *Geophysik III/Geophysics III, Handbuch der Physik/Encyclopedia of Physics*, pp. 547–602, Springer, Berlin.
- Matsushita, S. (1967b), Solar quiet and lunar daily variation fields, in *Physics of Geomagnetic Phenomena*, edited by S. Matsushita and W. H. Campbell, pp. 301–424, Academic Press, New York.
- Matsushita, S., and H. Maeda (1965), On the geomagnetic lunar daily variation field, *J. Geophys. Res.*, *70*, 2559–2578.
- Maute, A., B. G. Fejer, J. M. Forbes, X. Zhang, and V. Yudin (2016), Equatorial vertical drift modulation by the lunar and solar semidiurnal tides during the 2013 sudden stratospheric warming, *J. Geophys. Res. Space Physics*, *121*, 1658–1668, doi:10.1002/2015JA022056.
- Niu, X., J. Xiong, W. Wan, B. Ning, L. Liu, R. A. Vincent, and I. M. Reid (2005), Lunar tidal winds in the mesosphere over Wuhan and Adelaide, *Adv. Space Res.*, *36*, 2218–2222.
- Otsuka, Y., T. Ogawa, A. Saito, T. Tsugawa, S. Fukao, and S. Miyazaki (2002), A new technique for mapping of total electron content using GPS network in Japan, *Earth Planets Space*, *54*(1), 63–70, doi:10.1186/BF03352422.
- Paulino, A. R., P. P. Batista, and B. R. Clemesha (2012a), Lunar tides in the mesosphere and lower thermosphere over Cachoeira Paulista (22.7°S; 45.0°W), *J. Atmos. Sol. Terr. Phys.*, *78–79*, 31–36, doi:10.1016/j.jastp.2011.04.018.
- Paulino, A. R., P. P. Batista, B. R. Clemesha, R. A. Buriti, and N. Schuch (2012b), An enhancement of the lunar tide in the MLT region observed in the Brazilian sector during 2006 SSW, *J. Atmos. Sol. Terr. Phys.*, *90*, 97–103, doi:10.1016/j.jastp.2011.12.015.
- Paulino, A. R., P. P. Batista, and I. S. Batista (2013), A global view of the atmospheric lunar semidiurnal tide, *J. Geophys. Res. Atmos.*, *118*, 13,128–13,139, doi:10.1002/2013JD019818.
- Paulino, A. R., P. P. Batista, L. M. Lima, B. R. Clemesha, R. A. Buriti, and N. Schuch (2015), The lunar tides in the mesosphere and lower thermosphere over Brazilian sector, *J. Atmos. Sol. Terr. Phys.*, *133*, 129–138, doi:10.1016/j.jastp.2015.08.011.
- Pedatella, N. M. (2014), Observations and simulations of the ionospheric lunar tide: Seasonal variability, *J. Geophys. Res. Space Physics*, *119*, 5800–5806, doi:10.1002/2014JA020189.
- Pedatella, N. M., and J. M. Forbes (2010), Global structure of the lunar tide in ionospheric total electron content, *Geophys. Res. Lett.*, *37*, L06103, doi:10.1029/2010GL042781.
- Pedatella, N. M., and A. Maute (2015), Impact of the semidiurnal lunar tide on the midlatitude thermospheric wind and ionosphere during sudden stratosphere warmings, *J. Geophys. Res. Space Physics*, *120*, 10,740–10,753, doi:10.1002/2015JA021986.
- Pedatella, N. M., H.-L. Liu, and A. D. Richmond (2012a), Atmospheric semidiurnal lunar tide climatology simulated by the Whole Atmosphere Community Climate Model, *J. Geophys. Res.*, *117*, A06327, doi:10.1029/2012JA017792.
- Pedatella, N. M., H.-L. Liu, A. D. Richmond, A. Maute, and T.-W. Fang (2012b), Simulations of solar and lunar tidal variability in the mesosphere and lower thermosphere during sudden stratosphere warmings and their influence on the low-latitude ionosphere, *J. Geophys. Res.*, *117*, A08326, doi:10.1029/2012JA017858.
- Sabine, E. (1847), On the lunar atmospheric tide at St. Helena, *Philos. Trans. R. Soc.*, *137*, 45–50.
- Sandford, D. J., and N. J. Mitchell (2007), Lunar tides in the mesosphere over Ascension Island (8°S, 14.4°W), *Ann. Geophys.*, *25*, 9–12.
- Sandford, D. J., N. J. Mitchell, R. A. Vincent, and D. J. Murphy (2007), The lunar tides in the Antarctic mesosphere and lower thermosphere, *J. Atmos. Sol. Terr. Phys.*, *69*, 2219–2237.

- Stening, R. J. (2011), Lunar tide in the equatorial electrojet in relation to stratospheric warmings, *J. Geophys. Res.*, *116*, A12315, doi:10.1029/2011JA017047.
- Stening, R. J., and B. G. Fejer (2001), Lunar tide in the equatorial *F* region vertical ion drift velocity, *J. Geophys. Res.*, *106*, 221–226.
- Stening, R. J., and R. A. Vincent (1989), A measurement of lunar tides in the mesosphere at Adelaide, South Australia, *J. Geophys. Res.*, *94*, 10,121–10,129.
- Stening, R. J., S. K. Avery, and D. Tetenbaum (1990), Observations of lunar tides in upper atmosphere winds at Poker Flat, Alaska, *J. Atmos. Terr. Phys.*, *52*, 715–721.
- Stening, R. J., A. H. Manson, C. E. Meek, and R. A. Vincent (1994), Lunar tidal winds at Adelaide and Saskatoon at 80 to 100 km heights: 1985–1990, *J. Geophys. Res.*, *99*, 13,273–13,280.
- Stening, R. J., T. Tsuda, and T. Nakamura (2003), Lunar tidal winds in the upper atmosphere over Jakarta, *J. Geophys. Res.*, *108*, 1192, doi:10.1029/2002JA009528.
- Takahashi, H., et al. (2014), Diagnostics of equatorial and low latitude ionosphere by TEC mapping over Brazil, *Adv. Space Res.*, *54*(3), 385–394, doi:10.1016/j.asr.2014.01.032.
- Takahashi, H., C. Wrasse, Y. Otsuka, A. Ivo, V. Gomes, I. Paulino, A. Medeiros, C. Denardini, N. Sant'Anna, and K. Shiokawa (2015), Plasma bubble monitoring by TEC map and 630 nm airglow image, *J. Atmos. Sol. Terr. Phys.*, *130*, 151–158, doi:10.1016/j.jastp.2015.06.003.
- Takahashi, H., et al. (2016), Ionospheric TEC weather map over South America, *Space Weather*, *14*, 937–949, doi:10.1002/2016SW001474.
- Tarpley, J. D. (1971), The  $O_1$  component of the geomagnetic lunar daily variation, *J. Geomagn. Geoelectric.*, *23*(2), 169–179, doi:10.5636/jgg.23.169.
- Tarpley, J. D., and S. Matsushita (1971), The lunar tide in fbEs, *Radio Sci.*, *6*, 191–196.
- Tarpley, J. D., and S. Matsushita (1972), Lunar influences on sporadic *E*, *Radio Sci.*, *7*, 411–416.
- Vial, F., and J. M. Forbes (1994), Monthly simulations of the lunar semi-diurnal tide, *J. Atmos. Terr. Phys.*, *56*, 1591–1607.
- Wright, R. W., and N. J. Skinner (1959), Lunar tides in the sporadic *E*-layer at Ibadan, *J. Atmos. Terr. Phys.*, *13*, 217–221.
- Yamazaki, Y. (2013), Large lunar tidal effects in the equatorial electrojet during northern winter and its relation to stratospheric sudden warming events, *J. Geophys. Res. Space Physics*, *118*, 7268–7271, doi:10.1002/2013JA019215.
- Zhang, X., and J. M. Forbes (2014), Lunar tide in the thermosphere and weakening of the northern polar vortex, *Geophys. Res. Lett.*, *41*, 8201–8207, doi:10.1002/2014GL062103.